Electronic Supplementary Material (ESI) for Journal of Materials Chemistry A.

Supporting Information

Direct Growth and Post−Treatment of Zeolitic Imidazolate Framework-67 on Carbon Paper: Effective and Stable Electrode System for Electrocatalytic Reaction

*Anh Ngoc Nguyen, Ngoc Minh Tran, and Hyojong Yoo**

Department of Materials Science and Chemical Engineering, Hanyang University, Ansan, Gyeonggi-do, 15588, Republic of Korea

*Correspondence to: hjhaha73@hanyang.ac.kr

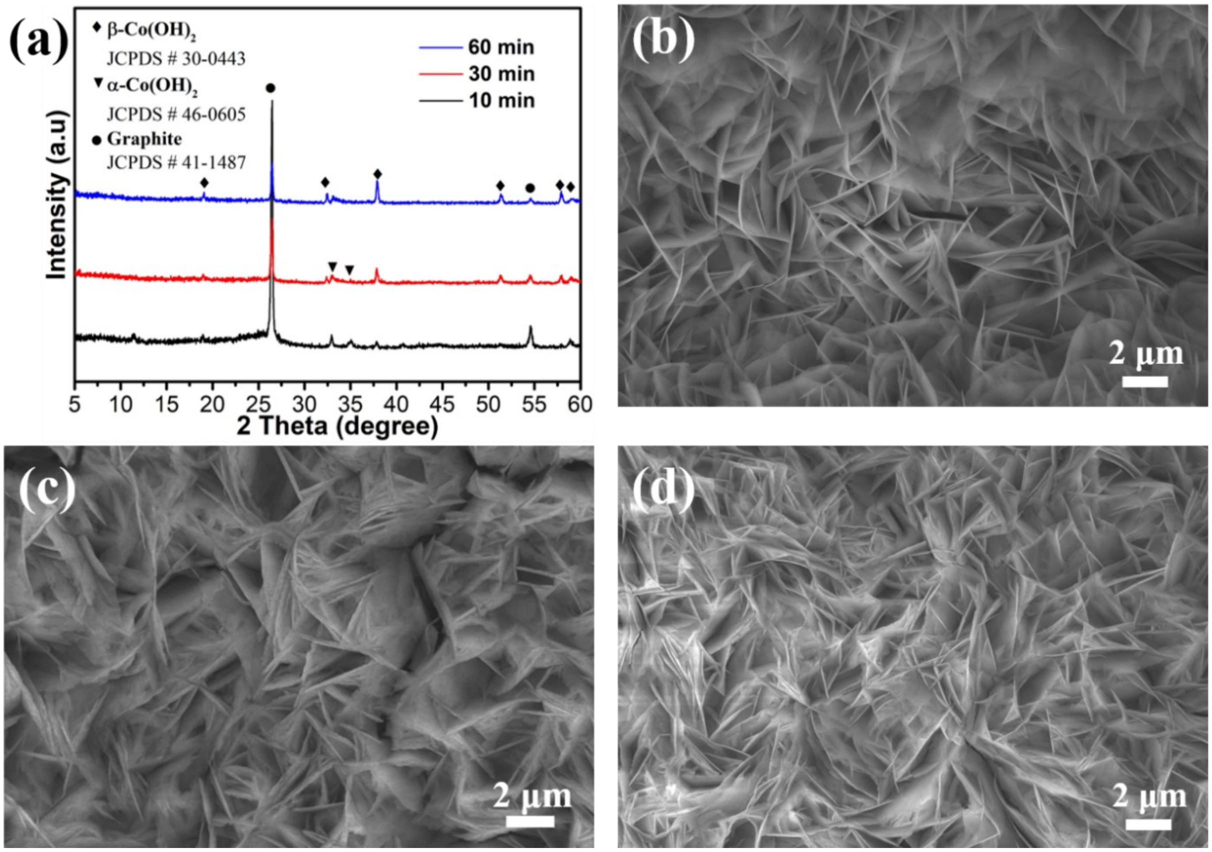

Figure S1. (a) XRD patterns and (b-d) SEM images of $Co(OH)_2$/CP samples with varied electrodeposition time, including (b) 10 minutes, (c) 30 minutes, (d) 60 minutes.

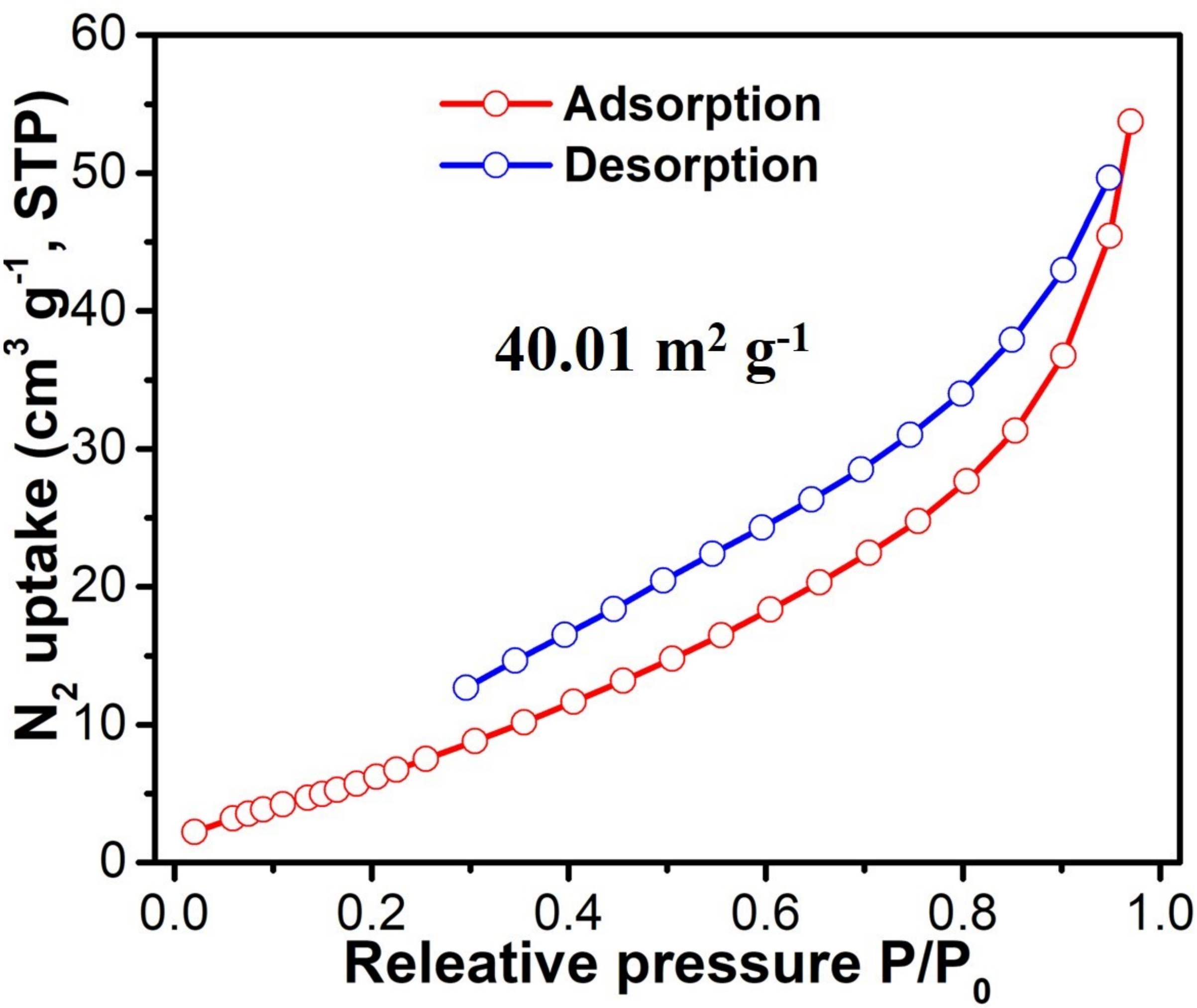

Figure S2. Nitrogen sorption measurement of CS@CH/CP 0.3.

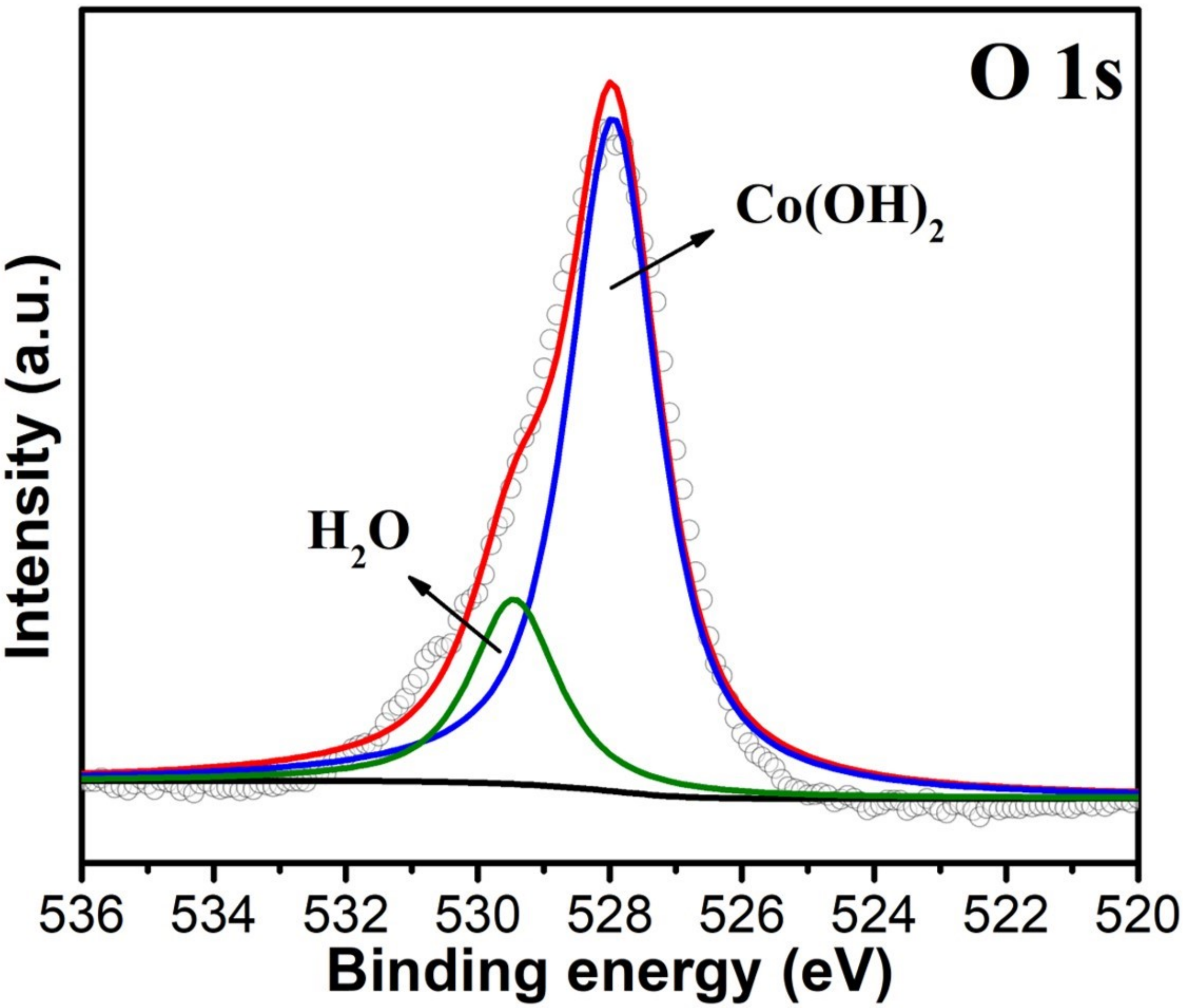

Figure S3. High-resolution XPS spectrum for O 1s of CS@CH/CP 0.3.

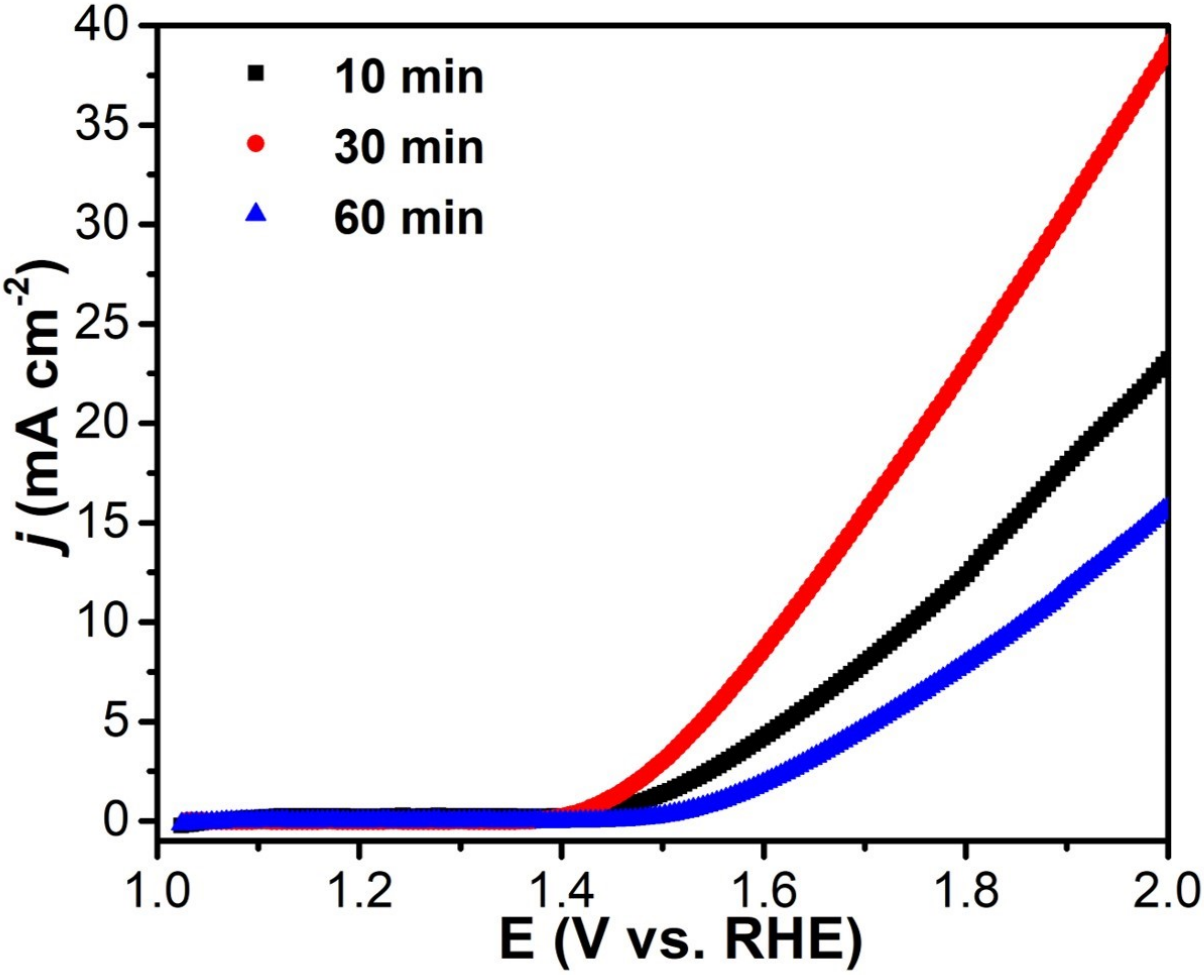

Figure S4. OER polarization of $Co(OH)_2$/CP with different electrodeposition time of 10, 30, and 60 minutes.

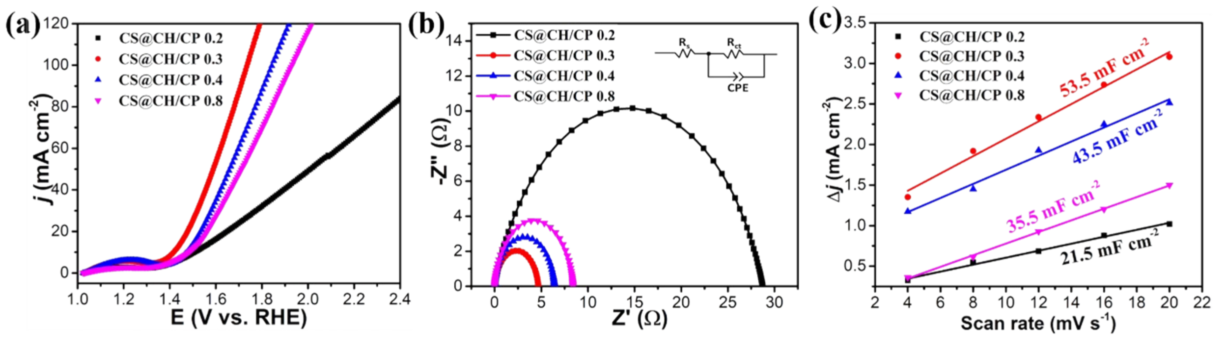

Figure S5. (a) OER polarization curves, (b) EIS profiles, and (c) C_{dl} values for CS@CH/CP samples etched with different thioacetamide concentrations, including 0.2 M, 0.3 M, 0.4 M, and 0.8M.

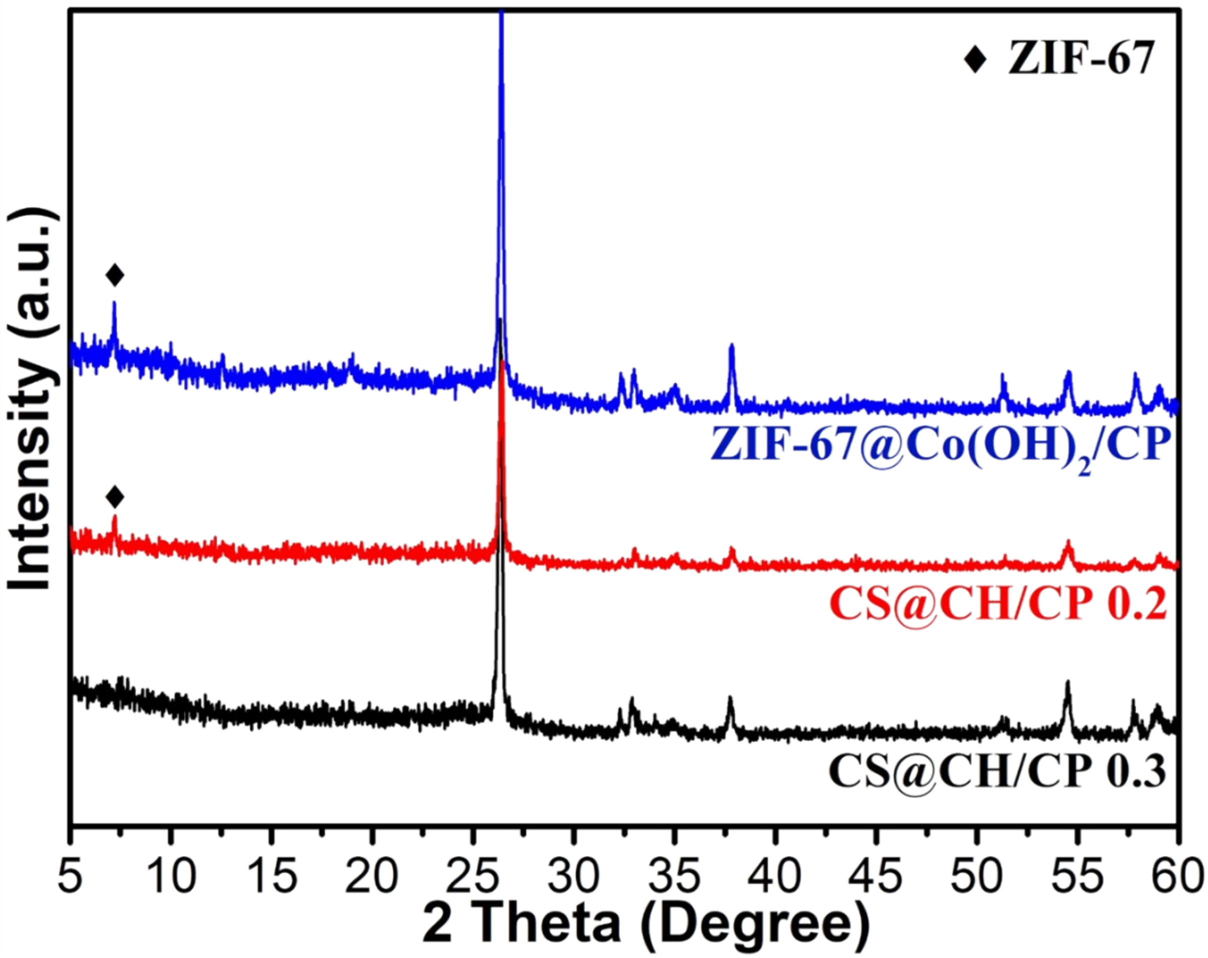

Figure S6. XRD patterns of ZIF-67@Co$(OH)_2$/CP, CS@CH/CP 0.2, and CS@CH/CP 0.3.

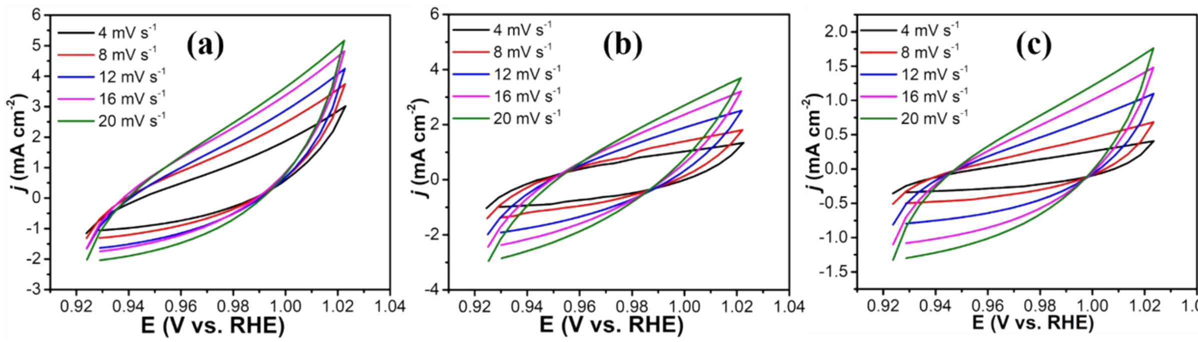

Figure S7. CV curves of CS@CH/CP etched with different thioacetamide concentrations: (a) 0.3 M, (b) 0.4 M and (c) 0.8 M.

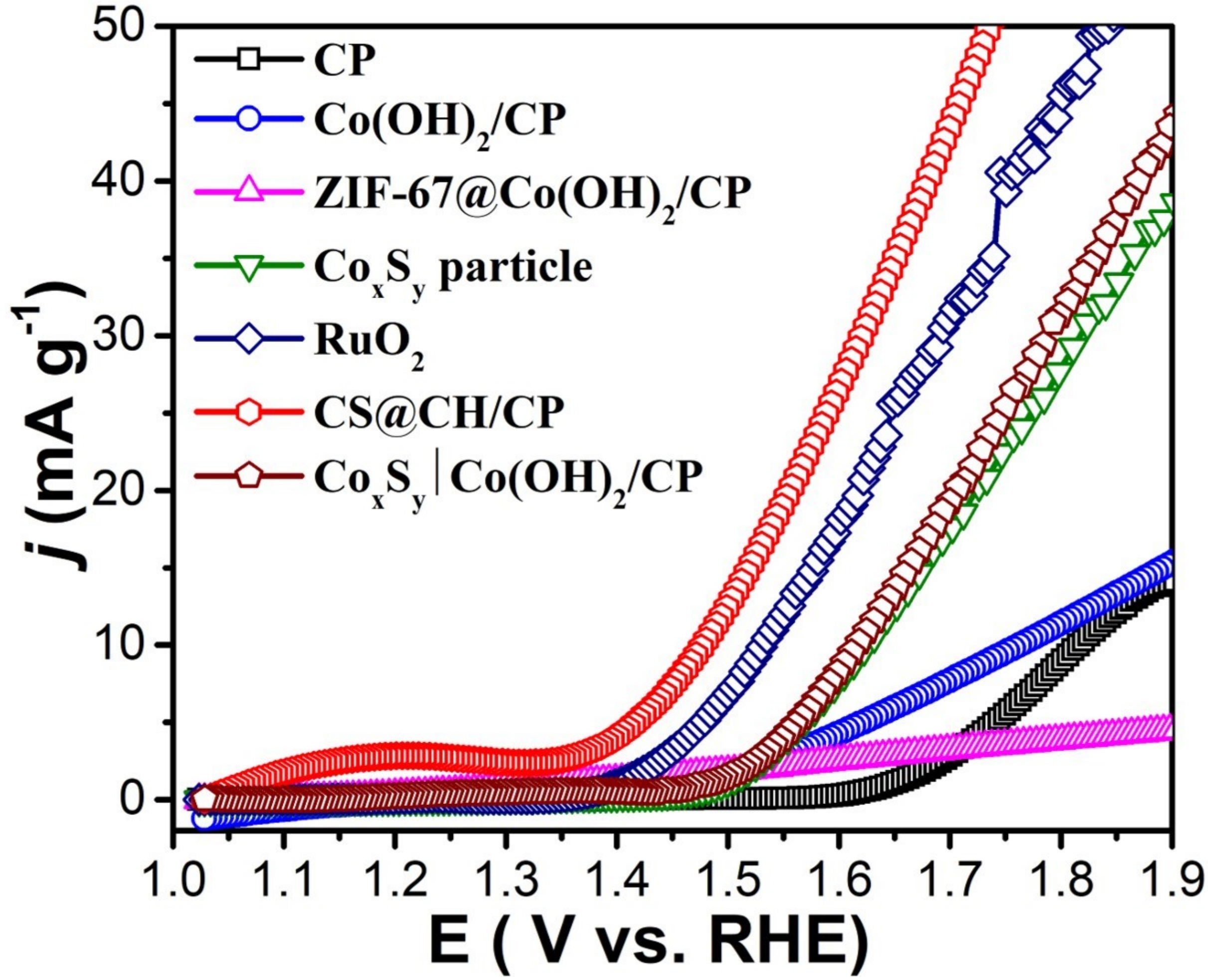

Figure S8. Mass normalized OER polarization curves of CP, $Co(OH)_2$/CP, ZIF-67@$Co(OH)_2$/CP, Co_xS_y particle, RuO_2, CS@CH/CP, and Co_xS_y|$Co(OH)_2$/CP

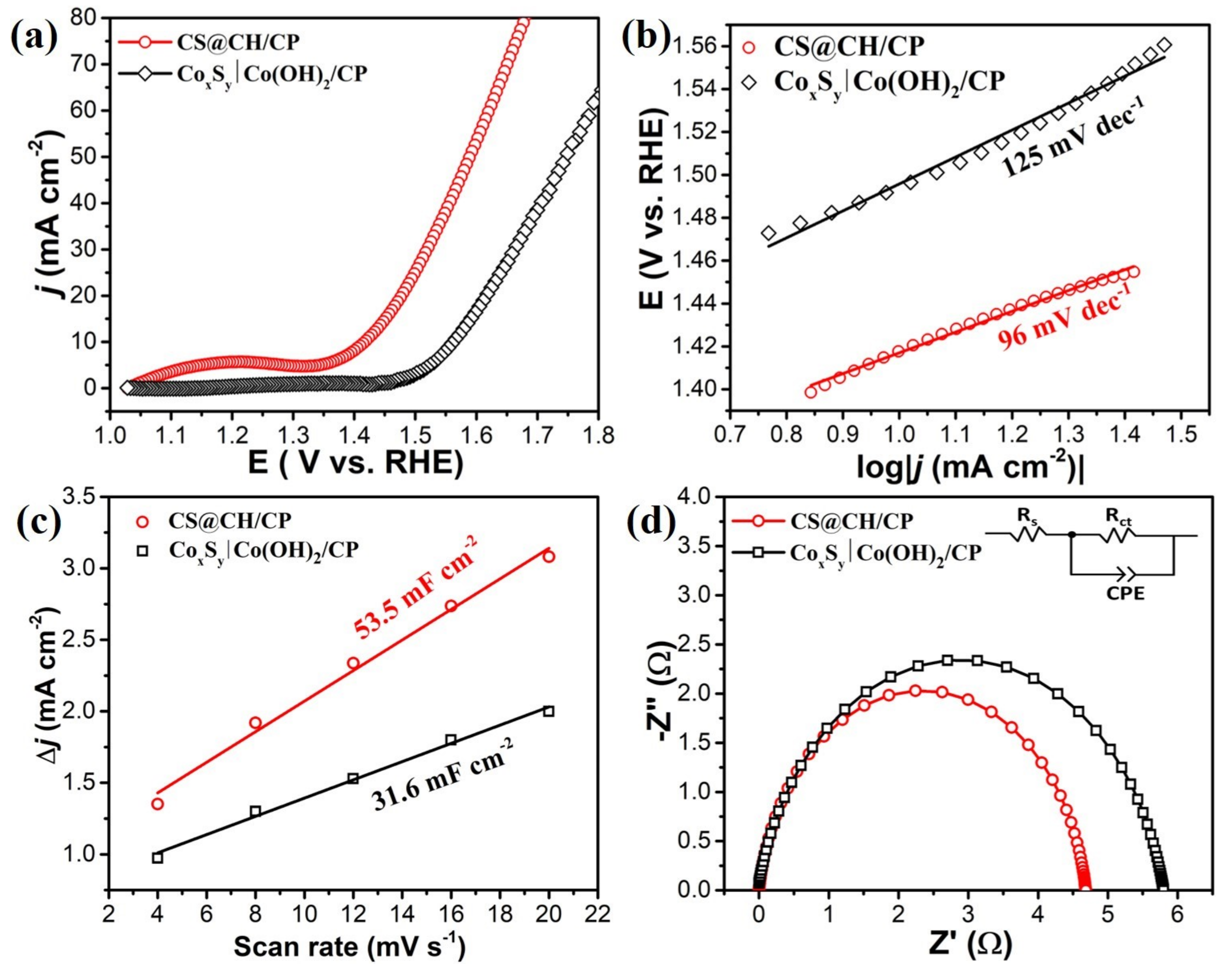

Figure S9. Polarization curves of OER performance with CS@CH/CP and $Co_xS_y|Co(OH)_2$/CP in N_2-saturated 1.0 M KOH solution: (a) OER polarization curves, (b) Tafel slopes, (c) Cdl values, (d) EIS profiles in the frequency range of 10^5 – 0.01 Hz at 0.75 V.

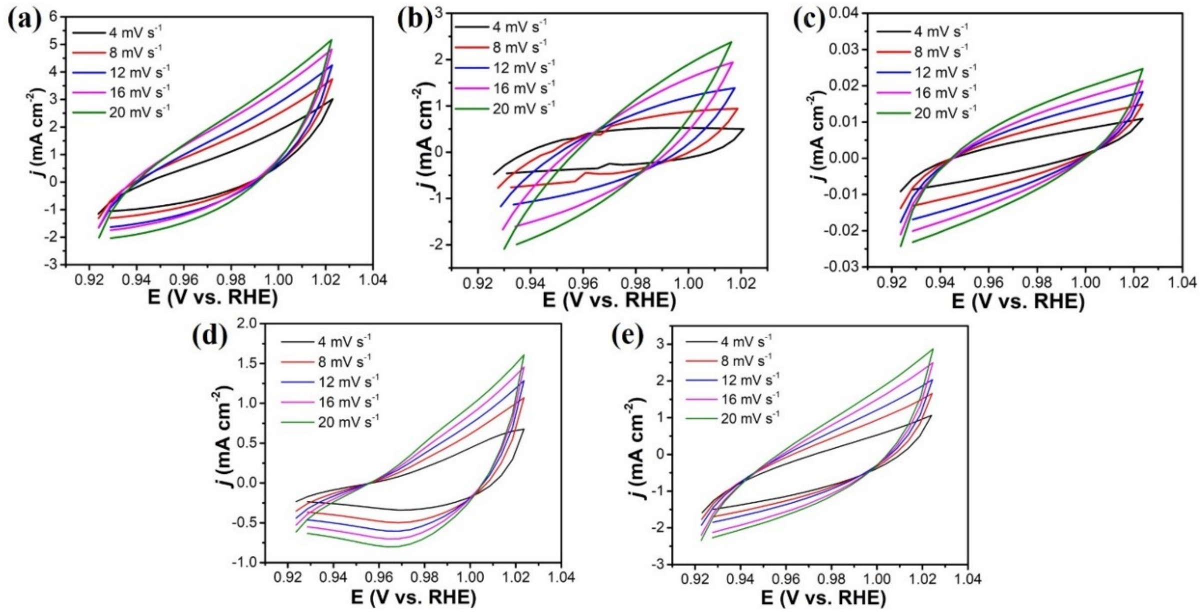

Figure S10. CV curves of (a) CS@CH/CP, (b) $Co(OH)_2$/CP, (c) CP, (d) Co_xS_y particle, and (e) Co_xS_y|$Co(OH)_2$/CP at elevated scan rate of 4, 8, 12, 16, and 20 mV s^{-1}.

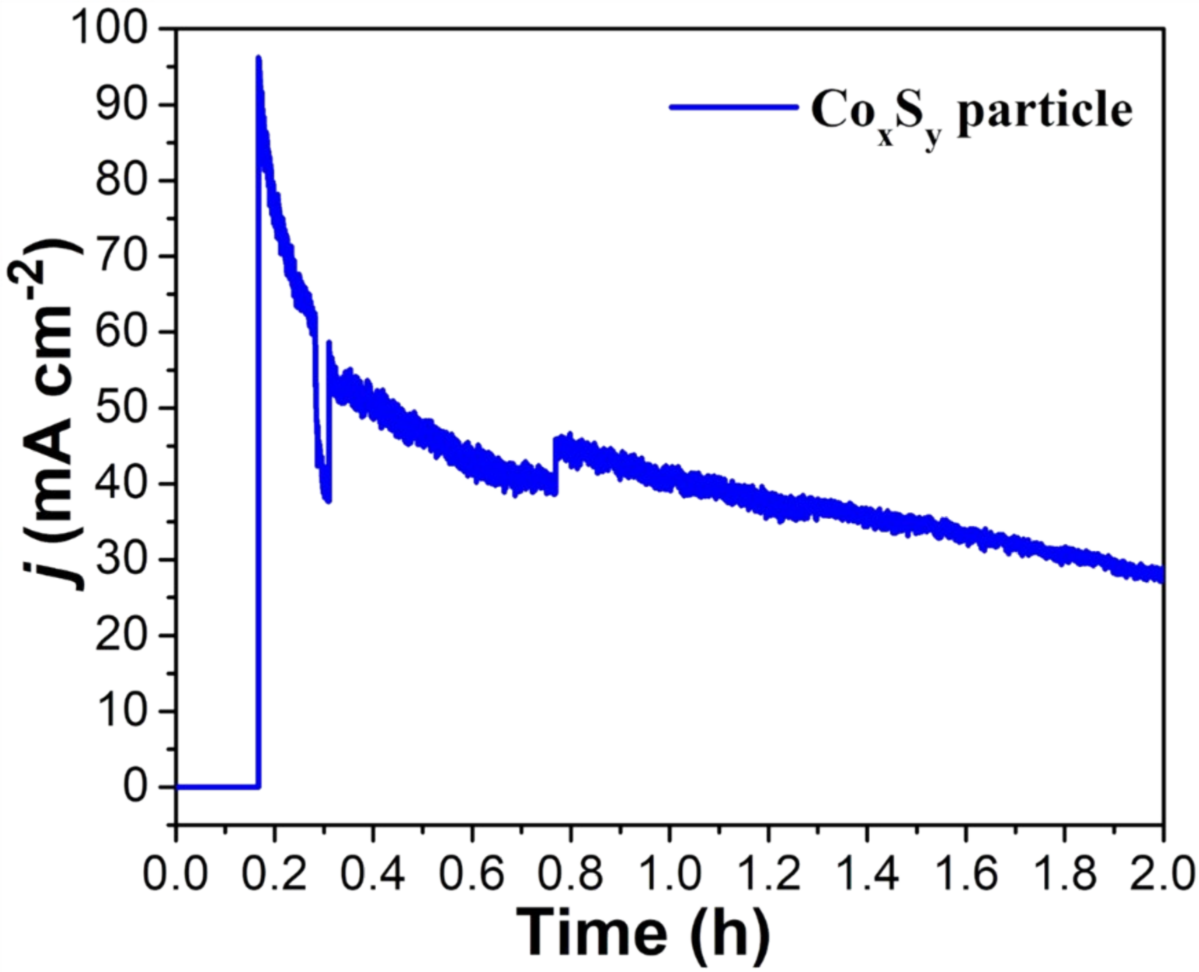

Figure S11. Current density–time curve of Co_xS_y particle.

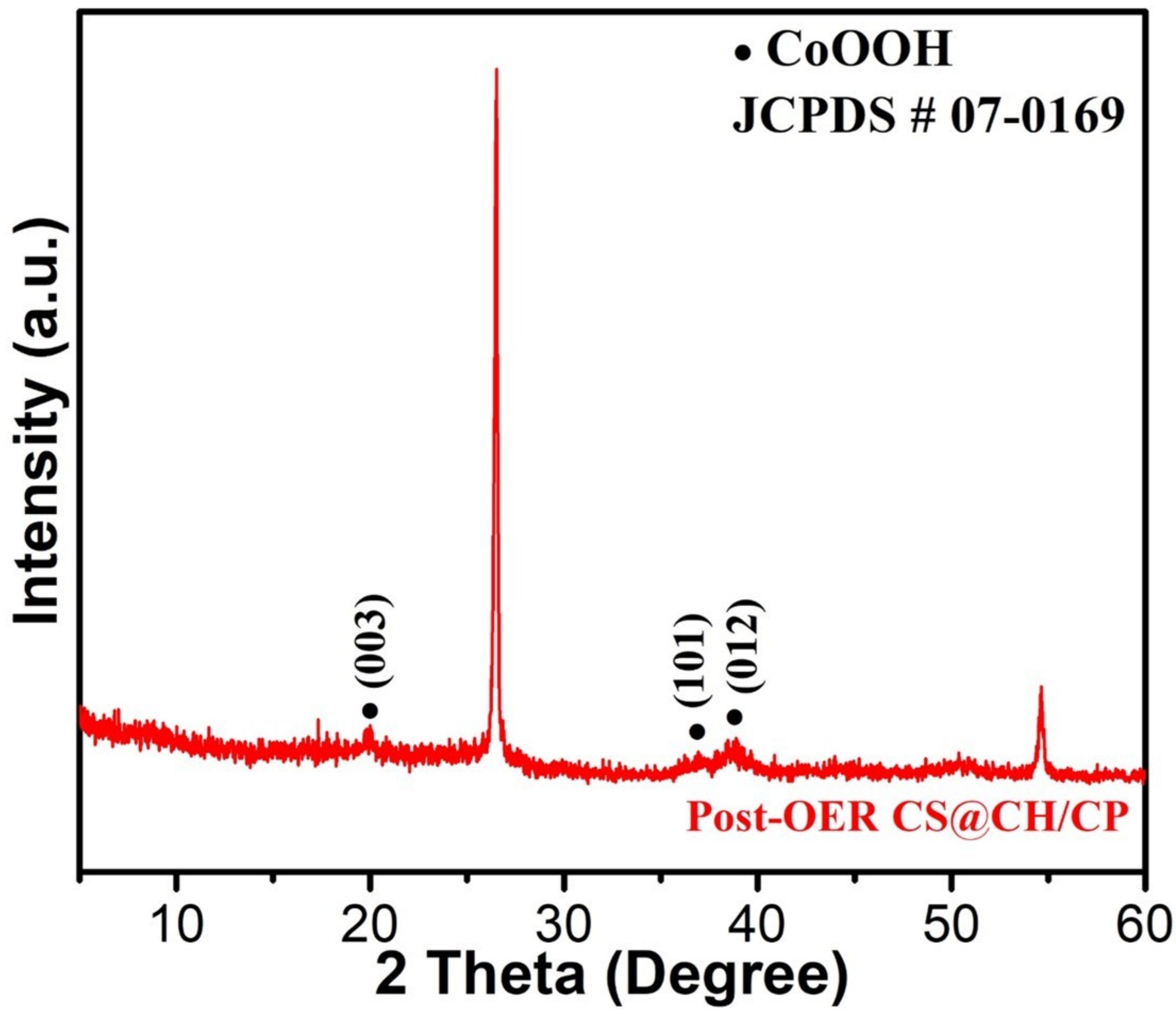

Figure S12. XRD pattern of CS@CH/CP after the stability test.

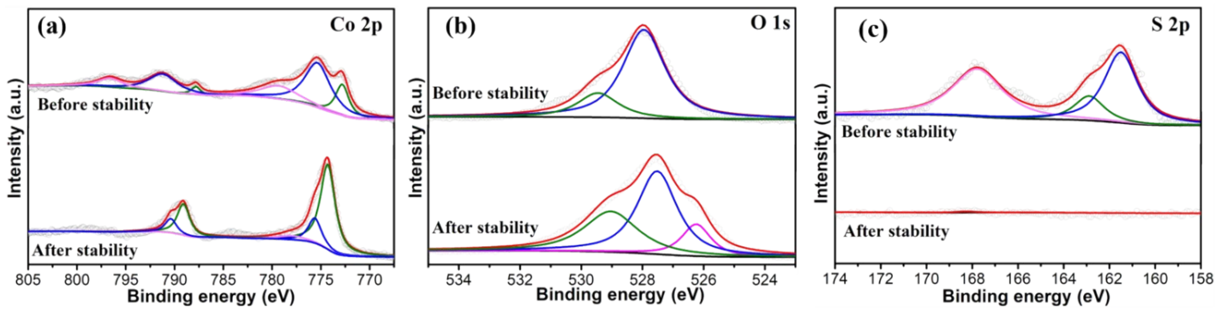

Figure S13. High-resolution XPS spectra for (a) Co 2p, (b) O 1s, and (c) S 2p in CS@CH/CP catalyst before and after the stability test.

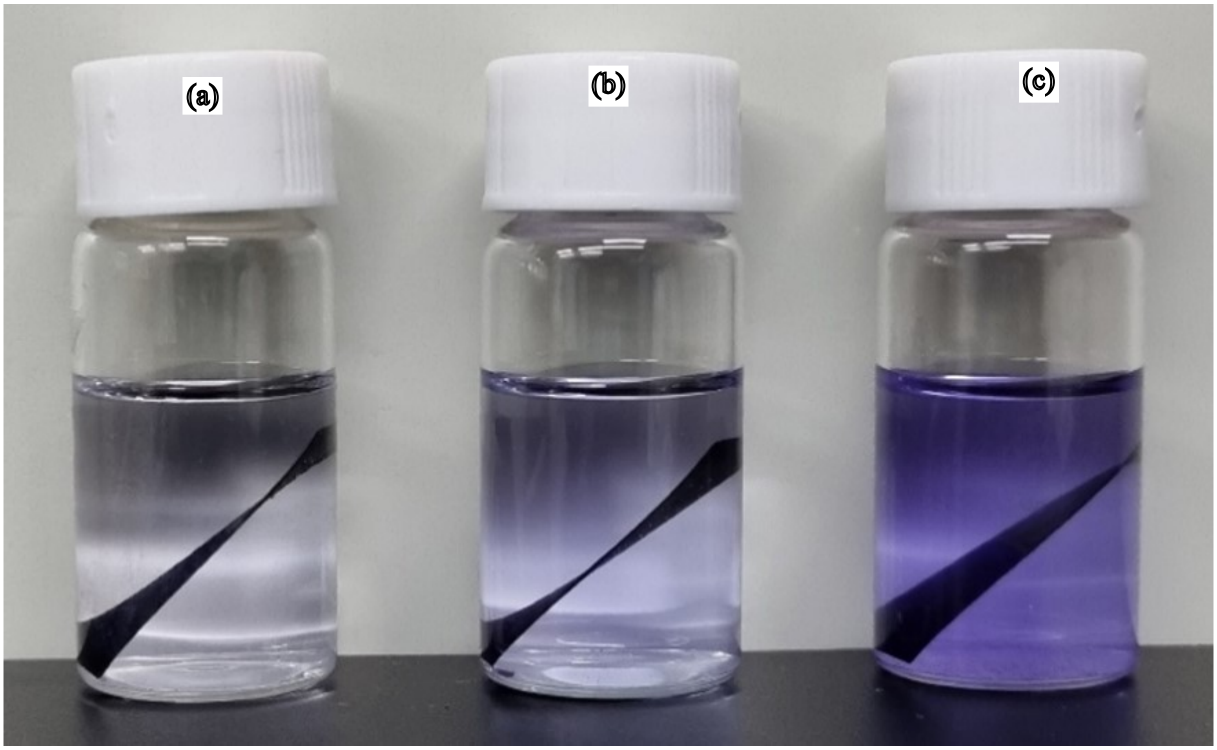

Figure S14. Digital images recording the growth of (a) ZIF-67(0.5)@$Co(OH)_2$/CP , (b) ZIF-67(1.0)@$Co(OH)_2$/CP , and (c) ZIF-67(2.0)@$Co(OH)_2$/CP.

Table S1. Comparison of OER performance of Co-containing electrocatalysts.

Catalyst	Substrate	Overpotential at 10 mA cm^{-2}	Tafel slope (mV dec^{-1})	Refs
$Ni_{2.3\%}$-CoS_2/CC	Carbon cloth	270 mV	119	1
CP/CTs/Co-S	Carbon paper	306 mV	72	2
CoP_3 NSs/CC	Carbon cloth	291 mV	72	3
Zn-Co-S NS/CFP	Carbon paper	390 mV	136	4
Zn-Co-S NP/CFP	Carbon paper	330 mV	97	4
Zn-Co-S NN/CFP	Carbon paper	320 mV	55	4
P-CoMoS/CC	Carbon cloth	260 mV	70.2	5
CoS_2/CC	Carbon cloth	290 mV	67	6
$NiCo_2S_4$/CC	Carbon cloth	240 mV	90.9	7
$CuCo_3S_z$/CC	Carbon cloth	346 mV (at 50 mA cm^{-2})	127	8
CoS_2	Carbon cloth	350 mV	107	9
$NiCo_2S_4$@Co_1Ni_4-LDH/CC	Carbon cloth	337 mV (at 100 mA cm^{-2})	111.2	10
S-NiCoP/CC	Carbon cloth	320 mV (at 20 mA cm^{-2})	150	11
h-Co_xS_y	Glassy carbon	320 mV	98	12
Co_9S_8@Co_3O_4/NF	Nickel foam	331 mV (at 100 mA cm^{-2})	65.5	13
Co_9S_8/CC	Carbon cloth	312 mV	127	14
Co_9S_8/Co@CC	Carbon cloth	265 mV	77.96	15
FeCoNiP	Glassy carbon	200 mV	~70	16
NiCo-UMOFNs	Copper foam	189 mV	42	17
CS@CH/CP	Carbon paper	180 mV	96	This work

Table S2: Elemental composition of CS@CH/CP 0.2, 0.3, 0.4, 0.8.

Sample	S wt% (Norm.)	Co wt% (Norm.)
CS@CH/CP 0.2	20.01	54.78
CS@CH/CP 0.3	26.90	47.90
CS@CH/CP 0.4	31.45	46.14
CS@CH/CP 0.8	41.26	40.14

Turnover frequency (TOF) calculation:

$$TOF = \frac{J \times A}{4 \times F \times n}$$

Where J is current density (A cm^{-2}), A is the geometry surface area of the electrode with the loaded catalyst, F is Faraday constant (96 500 A s mol^{-1}), and n is the total mole of active Co^{+2} in the catalyst. Assuming that all metal ions are active.

Geometrical area of electrode = 1 cm^2

Mass of loading catalyst = 2 mg cm^{-2}

→ Mass of loading catalyst on 1 cm^2 electrode = 2 mg

For CS@CH/CP 0.3,

Co wt% (based on EDX result in Table S2) = 47.90 wt%

Current density at $\eta_{300\ mV}$ = 45 mA cm^{-2}

→ Total mole of Co in the catalyst = 1.60 x 10^{-5} (mol)

→ TOF (at the overpotential of 300 mV) = $\frac{45 \times 10^{-3}\, A\, cm^{-2} \times 1\, cm^2}{4 \times 96485\, A\, s\, mol^{-1} \times 1.60 \times 10^{-5}\, mol}$ = 0.0073 s^{-1}

Using the same calculation, the TOF values of CS@CH/CP 0.2, CS@CH/CP 0.4, CS@CH/CP 0.8; $Co(OH)_2$/CP; RuO_2 and CoS particle are 0.0011; 0.0050; 0.0036; 0.0006; 0.0041; and 0.0008 s^{-1}, respectively.

REFERENCES

1 W. Fang, D. Liu, Q. Lu, X. Sun and A. M. Asiri, *Electrochem. commun.*, 2016, **63**, 60–64.

2 J. Wang, H. X. Zhong, Z. L. Wang, F. L. Meng and X. B. Zhang, *ACS Nano*, 2016, **10**, 2342–2348.

3 T. Wu, M. Pi, X. Wang, W. Guo, D. Zhang and S. Chen, *J. Alloys Compd.*, 2017, **729**, 203–209.

4 X. Wu, X. Han, X. Ma, W. Zhang, Y. Deng, C. Zhong and W. Hu, *ACS Appl. Mater. Interfaces*, 2017, **9**, 12574–12583.

5 C. Ray, S. C. Lee, K. V. Sankar, B. Jin, J. Lee, J. H. Park and S. C. Jun, *ACS Appl. Mater. Interfaces*, 2017, **9**, 37739–37749.

6 Y. H. Deng, C. Ye, B. X. Tao, G. Chen, Q. Zhang, H. Q. Luo and N. B. Li, *J. Power Sources*, 2018, **397**, 44–51.

7 W. Zhu, M. Ren, N. Hu, W. Zhang, Z. Luo, R. Wang, J. Weng, L. Huang, Y. Suo and J. Wang, *ACS Sustain. Chem. Eng.*, 2018, **6**, 5011–5020.

8 C. Mahala, R. Sharma, M. D. Sharma and S. Pande, *ChemElectroChem*, 2019, **6**, 5301–5312.

9 J. Zhang, X. Bai, T. Wang, W. Xiao, P. Xi, J. Wang, D. Gao and J. Wang, *Nano-Micro Lett.*, 2019, **11**, 1–13.

10 F. Yuan, J. Wei, G. Qin and Y. Ni, *J. Alloys Compd.*, 2020, **830**, 154658.

11 L. N. Mai-Thi, N. V. Hoang-Thy and Q. B. Bui, *Mater. Chem. Phys.*, 2021, **270**, 124746.

12 Z. Zhang, S. Li, X. Bu, Y. Dai, J. Wang, X. Bao and T. Wang, *New J. Chem.*, 2021, **45**, 17313–17319.

13 X. Wang, Y. He, X. Han, J. Zhao, L. Li, J. Zhang, C. Zhong, Y. Deng and W. Hu, *Nano Res.*, 2022, **15**, 1246–1253.

14 C. Zhan, Z. Liu, Y. Zhou, M. Guo, X. Zhang, J. Tu, L. Ding and Y. Cao, *Nanoscale*, 2019, **11**, 3193–3199.

15 Z. Nie, T. Liu, Y. Chen, P. Liu, Y. Zhang, Z. Fan, H. He, S. Chen and F. Zhang,

Electrochim. Acta, 2022, **402**, 139558.

16 J. Xu, J. Li, D. Xiong, B. Zhang, Y. Liu, K. H. Wu, I. Amorim, W. Li and L. Liu, *Chem. Sci.*, 2018, **9**, 3470–3476.

17 S. Zhao, Y. Wang, J. Dong, C. T. He, H. Yin, P. An, K. Zhao, X. Zhang, C. Gao, L. Zhang, J. Lv, J. Wang, J. Zhang, A. M. Khattak, N. A. Khan, Z. Wei, J. Zhang, S. Liu, H. Zhao and Z. Tang, *Nat. Energy*, 2016, **1**, 1–10.